Vision Research 101 (2014) 94–107

Contents lists available at ScienceDirect

Vision Research

journal homepage: www.elsevier.com/locate/visres

The 3-dimensional, 4-channel model of human visual sensitivity to grayscale scrambles

Andrew E. Silva [a], Charles Chubb [b,*]

[a] Department of Psychology, UCLA, United States
[b] Department of Cognitive Sciences, UC Irvine, Irvine, CA 92697-5100, United States

ARTICLE INFO

Article history:
Received 4 December 2013
Received in revised form 12 May 2014
Available online 14 June 2014

Keywords:
Texture
Blackshot
Scrambles
Contrast
Search
Attention

ABSTRACT

Previous research supports the claim that human vision has three dimensions of sensitivity to grayscale scrambles (textures composed of randomly scrambled mixtures of different grayscales). However, the preattentive mechanisms (called here "field-capture channels") that confer this sensitivity remain obscure. The current experiments sought to characterize the specific field-capture channels that confer this sensitivity using a task in which the participant is required to detect the location of a small patch of one type of grayscale scramble in an extended background of another type. Analysis of the results supports the existence of four field-capture channels: (1) the (previously characterized) "blackshot" channel, sharply tuned to the blackest grayscales; (2) a (previously unknown) "gray-tuned" field-capture channel whose sensitivity is zero for black rising sharply to maximum sensitivity for grayscales slightly darker than mid-gray then decreasing to half-height for brighter grayscales; (3) an "up-ramped" channel whose sensitivity is zero for black, increases linearly with increasing grayscale reaching a maximum near white; (4) a (complementary) "down-ramped" channel whose sensitivity is maximal for black, decreases linearly reaching a minimum near white. The sensitivity functions of field-capture channels (3) and (4) are linearly dependent; thus, these four field-capture channels collectively confer sensitivity to a 3-dimensional space of histogram variations.

1. Introduction

The standard back pocket model of preattentive texture segmentation Chubb and Landy (1991) proposes that human vision comprises a battery of image transformations, each of which continuously registers the time-varying distribution across the visual field of a specific, spatially local image statistic. We shall refer to image transformations of this sort as "field-capture" channels to reflect the rapid, spatially parallel nature of the transformations they perform. It is useful to think of field-capture channels as "measuring the amounts of various kinds of visual substances present in the image" Adelson and Bergen (1991). From this point of view, the output of a field-capture channel can be seen as a neural image Robson (1980) that reflects the spatial distribution of a specific visual substance for further processing by higher level vision.

Field-capture channels are conceptually akin to the "feature maps" hypothesized to subserve visual search Treisman and Gelade (1980). However, the term "feature map" might be taken to suggest a process that flags (in an all-or-none fashion) the locations marked by some specific feature such as greenness or verticality; by contrast, we conceptualize a field-capture channel as a process likely to yield graded responses to a range of image properties that may not be definable in terms of any easily characterized feature.

1.1. Grayscale scrambles

The purpose of the current experiment is to analyze the field-capture channels in human vision that are differentially sensitive to a class of textures called grayscale scrambles. Several examples of grayscale scrambles are shown in Fig. 1.

A grayscale scramble consists of a densely packed array of small squares called "texels" (short for "texture elements"), each painted with a grayscale drawn from a fixed set Ω. (In our experiments Ω comprises 9 grayscales linearly increasing in luminance from black to white.) The *histogram* of a scramble is the probability distribution $p(\omega)$ that gives the proportion of different squares painted grayscale ω in the scramble. It will sometimes be convenient to

* Corresponding author. Fax: +1 949 824 2307.
E-mail address: cfchubb@uci.edu (C. Chubb).

http://dx.doi.org/10.1016/j.visres.2014.06.001
0042-6989/

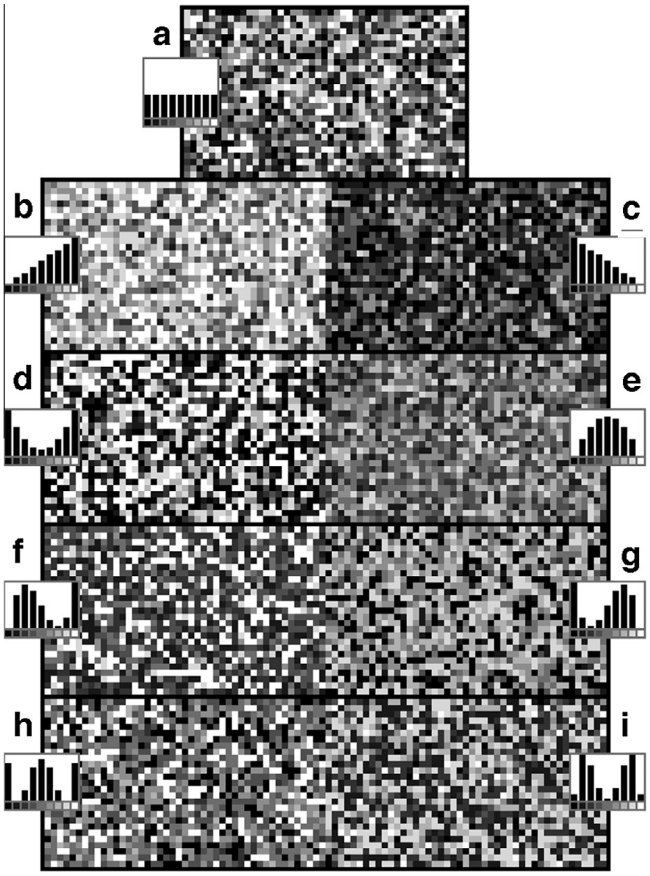

Fig. 1. *Examples of grayscale scrambles.* Scrambles with histograms (a) U, (b) $U+\lambda_1$, (c) $U-\lambda_1$, (d) $U+\lambda_2$, (e) $U-\lambda_2$ (f) $U+\lambda_3$, (g) $U-\lambda_3$, (h) $U+\lambda_4$, (i) $U-\lambda_4$. The inset in each patch of scramble gives the histogram of that scramble.

refer to a scramble with histogram p as a "p-scramble" (as in the following sentence). To generate a p-scramble comprising N spatial squares it suffices to

1. fill a virtual urn with N grayscales whose proportions conform to histogram p and then
2. assign these grayscales randomly from the urn without replacement.

The result is a spatially random texture with precisely the prescribed histogram p.[1]

It will be convenient to write U for the uniform histogram; i.e., $U(\omega)=\frac{1}{9}$ for all $\omega\in\Omega$. In addition, any function $\rho:\Omega\to\mathbb{R}$ is called a *perturbation* if $U+\rho$ and $U-\rho$ are both probability distributions. If the maximum absolute value of ρ is $\frac{1}{9}$, then for any scalar A greater than 1, either $U+A\rho$ or else $U-A\rho$ will fail to be a probability distribution; in this case, ρ is called *maximal*.

From the fact that $U+\rho$ is a probability distribution, it follows that

$$\sum_{\omega\in\Omega}\rho(\omega)=0. \tag{1}$$

Any function satisfying Eq. (1) is said to "sum to 0."

[1] Chubb, Econopouly and Landy (1994) used IID textures rather than grayscale scrambles. The difference between an IID texture vs a grayscale scramble is that grayscales are assigned in an IID texture *with* replacement rather than *without* replacement as they are in a grayscale scramble. The key difference between a patch of IID texture vs a patch of grayscale scramble is that the histogram of the IID patch is likely to deviate from the histogram p that characterizes the grayscales in the urn.

1.2. The sensitivity function of a field-capture channel

We will assume that any field-capture channel that is differentially sensitive to grayscale scrambles can be characterized by a sensitivity function

$$F(\omega)=C+f(\omega) \tag{2}$$

for some function $f:\Omega\to\mathbb{R}$ that sums to 0 and some scalar C sufficiently large that $F(\omega)\geqslant 0$ for all $\omega\in\Omega$. The constraint that F be nonnegative reflects an assumption that the baseline firing rate of the neurons used to implement any field-capture channel is 0 and that activation of the field-capture channel is signaled exclusively by firing rates increasing above this baseline level. The scalar C is called the *baseline constant* and the function f is called the sensitivity *modulator* of the field-capture channel.

Under this assumption, the space-average activation produced in the field-capture channel by a grayscale scramble with histogram p is equal to

$$F\bullet p=\sum_{\omega\in\Omega}F(\omega)p(\omega). \tag{3}$$

The difference in activation produced in the field-capture channel by scrambles with grayscale histograms p and q is $F\bullet p-F\bullet q=F\bullet\delta$ for $\delta=p-q$; however, because δ sums to 0, it is easily seen that $F\bullet\delta=f\bullet\delta$. Thus, the difference in activation produced in any field-capture channel by any two scrambles depends only on the sensitivity modulator of the field-capture channel (not on its baseline constant). Note in particular that if $p=U+\rho$ and $q=U-\rho$ for some perturbation ρ, then the difference in activation is $F\bullet(p-q)=2f\bullet\rho$.

1.3. The analogy to color perception

A useful analogy can be drawn to color perception. Under this analogy,

- texels of different grayscales correspond to quanta of different wavelengths,
- a scramble corresponds to a light,
- the histogram of the scramble corresponds to the spectrum of the light,
- a scramble-sensitive field-capture channel corresponds to a cone-class,
- the sensitivity function characterizing the field-capture channel corresponds to the sensitivity function characterizing the cone-class.

Let us flesh this analogy out in more detail and develop some of its implications. Human vision comprises three cone-classes, the S-cones, the M-cones and the L-cones, with sensitivity functions F_S, F_M and F_L. For any wavelength $w, F_S(w), F_M(w)$ and $F_L(w)$ reflect the activation produced in S-, M- and L-cones by quanta of wavelength w. The activations produced by a light with spectrum $H(w)$ in the S-, M- and L-cones are given by

$$\begin{aligned}F_S\bullet H&=\int F_S(w)H(w)dw,\quad F_M\bullet H\\&=\int F_M(w)H(w)dw,\quad\text{and}\quad F_L\bullet H=\int F_L(w)H(w)dw\end{aligned} \tag{4}$$

where each of the integrals is over all wavelengths w of electromagnetic radiation in the visible range (roughly 300–800 nm). Note that Eq. (4) is precisely analogous to Eq. (3) except that the summation in Eq. (3) has become an integral.

We assume, analogously, that human vision comprises some number N of scramble-sensitive field-capture channels with sensi-

tivity functions $F_1, F_2, \cdots, F_N$. For any grayscale $\omega, F_k(\omega)$ reflects the activation produced in the k^{th} of these field-capture channels by texels of grayscale ω. The activations produced by a grayscale scramble with histogram $p(\omega)$ in these N field-capture channels are

$$F_k \bullet p, \quad k = 1, 2, \ldots, N. \tag{5}$$

Lights with spectra H_1 and H_2 will appear identical to a human observer if

$$F_S \bullet H_1 = F_S \bullet H_2 \quad \text{and} \quad F_M \bullet H_1 = F_M \bullet H_2 \quad \text{and} \quad F_L \bullet H_1 = F_L \bullet H_2. \tag{6}$$

In this case the lights are said to be "metameric."

Analogously scrambles with histograms p_1 and p_2 will be "preattentively equivalent" to human vision if

$$F_k \bullet p_1 = F_k \bullet p_2 \quad \text{for } k = 1, 2, \ldots, N. \tag{7}$$

The modifier "preattentively" in the phrase "preattentively equivalent" is intended to indicate that even though no field-capture channels are differentially activated by the two scrambles, it may nonetheless be possible to use focal attention to identify a difference between the two textures. See Chubb et al. (in press) for a dramatic example of metameric grayscale scrambles.

The analogy to color perception breaks down in one respect. One can double the intensity of a light by doubling its quantal flux at each wavelength; it is impossible, however, to increase the number of texture elements in some fixed area. In this regard, grayscale scrambles are analogous to a space of lights whose spectra H may differ in the proportions of different wavelength quanta they contain but which are constrained to deliver to the eye the same fixed total number of quanta per unit time.

1.4. Previous studies investigating discrimination of grayscale scrambles

Although the current study will require us to amend this conclusion, a series of recent studies suggests that human vision has three distinct field-capture channels selectively sensitive to grayscale scrambles (Chubb, Econopouly & Landy, 1994; Chubb, Landy & Econopouly, 2004; Chubb, Nam, Bindman, & Sperling, 2007).

Let S be the space of all perturbations ρ for which the mean and variance of $U + \rho$ are equal to the mean and variance of U. Chubb, Econopouly and Landy (1994) showed that for any $\rho \in S$, the probability of correctly judging the orientation of a square wave whose bars alternated between scrambles with histograms $U + \rho$ vs $U - \rho$ was a psychometric function of $|\tilde{f} \bullet \rho|$ for a particular function $\tilde{f} \in S$. They concluded that:

1. Sensitivity to scrambles differing in qualities other than mean or variance is conferred primarily by a single field-capture channel.
2. One or the other of $\tilde{f}$ or $-\tilde{f}$ is the projection into S of the sensitivity modulator of this field-capture channel.

Chubb, Landy and Econopouly (2004) measured the sensitivity of this field-capture channel to variations in scramble mean and variance, determining the sensitivity function modulator up to an unknown sign. They discovered that this field-capture channel was highly sensitive to the relative proportions of scramble grayscales very near black (with Weber contrasts less than −0.9) but was uninfluenced by variations in the proportions of other grayscales. They called this field-capture channel the "blackshot" channel to reflect its sharp tuning to grayscale values very near black.

Estimates of the blackshot sensitivity functions for three observers are shown in Fig. 2. It should be noted, however, that the plots in Fig. 2 embody several assumptions that have not been definitively established by previous experiments. First, in assuming that the blackshot channel responds positively to grayscales near black, this figure assigns a sign to the modulator of the blackshot sensitivity function. Second, in assuming that the blackshot channel assigns values near 0 to grayscales other than black, Fig. 2 assigns a particular value to the baseline constant of the blackshot sensitivity function. The results of Chubb, Landy and Econopouly (2004) establish neither the sign of the blackshot sensitivity modulator nor the value of the blackshot baseline constant.

Chubb et al. (2007) sought to determine the number of field-capture channels in human vision that are differentially sensitive to grayscale scrambles. Their method hinged on the observation that if human vision contains N field-capture channels differentially sensitive to grayscale scrambles, then in any $N + 1$ dimensional space of perturbations, there must exist a maximal perturbation ρ for which the scrambles with histograms $U + \rho$ vs $U - \rho$ are perceptually equivalent and hence for which preattentive segregation is impossible. They tested five subspaces of perturbations: the subspace spanned by the 1st, 2nd, 3rd and 4th order Legendre polynomials (these are the perturbations $\lambda_1, \lambda_2, \lambda_3$ and λ_4 used to produce the histograms of the grayscale scrambles shown in Fig. 1) as well as each of the four subspaces spanned by a subset of three of these four polynomials. For each subspace, participants used an adjustment procedure to find the maximal perturbation ρ in the given subspace such that the perceptual difference between the scrambles with histograms $U + \rho$ and $U - \rho$ was as weak as possible. Each of the five resulting minimal salience perturbations ρ was then tested in a task in which the participant was required to detect the location of a target patch of scramble with histogram $U + \rho$ superimposed onto a background scramble with histogram $U - \rho$.

Chubb et al. (2007) found that only the minimal salience perturbation extracted from the subspace spanned by all four of $\lambda_1, \lambda_2, \lambda_3$ and λ_4 yielded chance performance in the location detection task; the minimal salience perturbations extracted from each of the four three-dimensional subspaces all yielded performance significantly greater than chance in the location detection task. They accounted for these findings by positing three field-capture channels differentially sensitive to grayscale scrambles: one channel sensitive primarily to mean scramble grayscale; another sensitive primarily to grayscale variance, and the third (blackshot) channel sensitive to grayscales very near black. However, they acknowledged that although the three field-capture channels they posited sufficed to account for their results, any set of field-capture channels with sensitivity functions spanning the same space would work just as well.

1.5. Open questions about grayscale scrambles

Little is known about the field-capture channels (other than the blackshot channel) implicated by the experiments of Chubb et al. (2007). The results of Chubb et al. (2007) support the conclusion that human vision has three dimensions of sensitivity to grayscale scrambles. Although it seems natural to jump from this observation to the conclusion that human vision comprises only three field-capture channels that are differentially sensitive to grayscale scrambles, this need not be true: it could be the case that human vision has more than three such field-capture channels; if so, however, then the sensitivity functions of these field-capture channels must be linearly dependent. In fact, the "3D4C" (3-dimensional, 4-channel) model used below to fit the data from the current experiment (Section 3.3) proposes a scenario of precisely this sort.

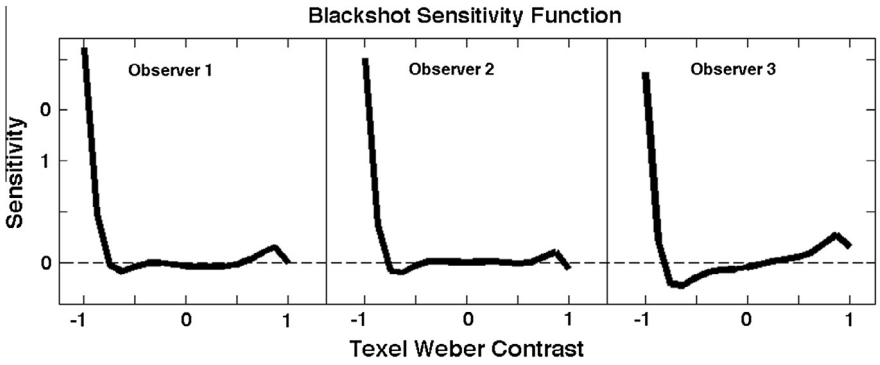

Fig. 2. *Blackshot sensitivity function.* The three functions shown give 7th order polynomial estimates of the blackshot sensitivity function for three different observers. It should be noted that previous experimental methods define the blackshot sensitivity function only up to arbitrary additive and multiplicative constants. These functions have been plotted under the assumption that the blackshot field-capture channel is activated by the darkest elements of the display (assigning a positive value to Weber contrast −1) and is otherwise silent (assigning values very close to "0" to all but the blackest elements).

Second, although it seems natural to assume that the blackshot channel is positively activated by texture elements with grayscales near black, previous experiments do not resolve the sign of the modulator of the blackshot sensitivity function. The main reason for this is that the task used in the previous experiments (a task requiring the participant to judge the orientation of a scramble-defined square wave grating) provides no traction in deciding whether the blackshot channel is more highly activated by spatial regions high in black elements or devoid of black elements.

1.6. Assumptions underlying the current experiments

Previous models offered to account for the results of experiments in preattentive texture discrimination (e.g., Chubb, Econopouly & Landy, 1994; Chubb, Landy & Econopouly, 2004; Chubb et al., 2007; Victor, Chubb & Conte, 2005) have assumed:

1. A given texture A operates in a bottom-up fashion to produce a vector α_A of activations in the different field-capture channels in human vision.
2. The salience of the difference between textures A vs B is given by some distance $D(\alpha_A, \alpha_B)$.
3. Probability correct in any choice task requiring the participant to discriminate textures A vs B is given by some psychometric function of $D(\alpha_A, \alpha_B)$.

Note that under this model, there is no room for top-down attention to influence performance in any given texture discrimination task. Nor does this model admit the possibility that performance can be influenced by swapping the spatial roles of textures A vs B within the stimulus. Consequently, previous experiments have tended to use paradigms in which different texture discrimination conditions were mixed within blocks (e.g., Victor, Chubb & Conte, 2005), the effect of which is to minimize any effects due to variations in the attentional state of the participant. Previous experiments have also tended to use stimulus displays in which the two textures to be discriminated on a given trial played spatially symmetric roles (e.g., Chubb, Econopouly & Landy, 1994), the effect of which is to insure that performance will be invariant with respect to swapping the roles of the textures A and B in the stimulus.

By contrast, the task used in the experiments reported here requires the participant to detect the location of a small patch of p-scramble in a large annular background of q-scramble; moreover, in a given, separately blocked condition, the histograms p and q are kept approximately constant to enable the participant to use top-down attention to optimize performance. For tasks of this sort, we submit that performance is likely to differ when the roles of the target and background scramble are reversed.

In particular, suppose (as the models considered in this paper assume) that the following conditions hold:

1. Any given field-capture channel can produce only nonnegative levels of activation.
2. The participant is able to use top-down attention to selectively recruit specific field-capture channels for performing searches of this sort.
3. Search is efficient only if the participant can combine input from his/her field-capture channels to produce a spatial "search map" in which neuronal activation is higher in the region of the target than it is in the background.[2]

Under assumptions 1, 2 and 3, if a given field-capture channel with sensitivity function F is useful for detecting a scramble target with histogram p in a background with histogram q, then it must be true that $F \bullet p > F \bullet q$ from which it follows that this field-capture channel will *not be useful* for detecting a target with histogram q in a background with histogram p. This observation implies that there should be no overlap between the field-capture channels

[2] In the annular displays used in the current experiments, if the participant can produce a search map that is more strongly activated by the target than by the background, then the location of the target will be signaled directly and naturally by the centroid of activation of the search map. There is ample evidence to support the claim that centroid extraction is a low-level visual computation used to localize targets in many contexts (Baud-Bovy & Soechting, 2001; Friedenberg & Liby, 2002; McGowan, Kowler, Sharma, & Chubb, 1998). On the other hand, if the region of the background is activated more strongly than the target in the search map, then the centroid of the pattern of activation in the search map is unlikely to be very useful to the participant in producing his/her response.

It might be argued that suppressed activation in the search map at the location of the target carries just as much information as elevated activation. There are two responses to this objection:

(a) If the pattern of activation produced by a scramble in a given field-capture channel were spatially homogeneous, then this contention might have some force; however, this is not the case. The response of a field-capture channel to a scramble will inevitably be variable across space, and the variance of this signal is likely to increase with mean activation. This means that the signal produced by a field-capture channel that is more highly activated by the background scramble than it is by the target scramble is likely to contain much less useful information (even for an ideal observer) than is the signal produced by a field-capture channel that is more highly activated by the target scramble than it is by the background scramble.

(b) It is undoubtedly true that the suppressed activation in the search map at the location of the target carries some potentially useful information; however, unless the visual system can convert the "hole" in search-map activation into a "bump" in activation in some other neural population, it is difficult to see how this information can be used to produce a response.

used by a participant in searching for a target with histogram p in a background with histogram q vs in searching for a target with histogram q in a background with histogram p. This makes it likely that the grayscale-sensitivities of the search maps produced in these two tasks will differ strongly.

2. Methods

2.1. Participants

There were three participants (one of whom was the first author). Each had normal or corrected-to-normal vision. The UC Irvine Institutional Review Board approved the experimental procedures, and all participants gave signed consent.

2.2. Equipment

An iMac desktop computer running OS X version 10.6.8 with a 3.06 GHz Intel Core 2 Duo processor and 4 GB memory capacity was used for stimuli presentation and data collection. The computer was equipped with an ATI Radeon HD 4670 graphics chip. The monitor had a resolution of 1920 × 1080 and a viewable diagonal measure of 21.5 inches.

2.3. Calibration

Linearization of the 9 grayscales used in the stimuli was achieved using a psychophysical adjustment procedure (used previously by Chubb, Econopouly & Landy (1994), Chubb, Landy & Econopouly (2004) and Chubb et al. (2007)) in which a regular grid of texture elements containing three intensities lum_{lo}, lum_{hi} and lum_{mid} (half with luminance lum_{mid}, $\frac{1}{4}$ with lum_{lo} and $\frac{1}{4}$ with lum_{hi}) alternated in a coarse vertical square-wave with texture comprising a checkerboard of texture elements alternating between intensities lum_{lo} and lum_{hi}. The screen was then viewed from sufficiently far away that the fine granularity of the texture was barely visible. At this distance, the square-wave modulating between the two types of texture had a spatial frequency of approximately 4 cycles per deg. Since the texture itself could not be resolved, the square-wave is visible only if the mean luminance of alternating texture bars is different. Thus, the luminance lum_{mid} (obtained by adjustment) that makes the square-wave vanish is equal to the average of the intensities lum_{lo} and lum_{hi}. We use the lights v_0 and v_8 produced by the minimal and maximal pixel values p_0 and p_8 of our monitor as the black and white grayscales in our set. We then use our adjustment procedure to derive in succession the pixel values (1) p_4 with luminance v_4 midway between v_0 and v_8, (2) p_2 with luminance v_2 midway between v_0 and v_4, and (3) p_1 with luminance midway between v_0 and v_2. We then fit a power function $f_{\alpha,\beta}(p_k) = \alpha p_k^{\beta}$ that minimizes the sum of $(f_{\alpha,\beta}(p_k) - v_k)^2$ over $k = 0, 1, 2, 4, 8$. (The fit is nearly exact.) We take as our nine grayscales the lights with pixel values $f^{-1}_{\alpha,\beta}(v_k), k = 0, 1, 2, \ldots, 8$. This procedure insures that grayscales are linearized in the same sorts of contexts as those in which they will occur in the stimuli, minimizing distortions due to any spatial nonlinearities in the display.

2.4. The structure of a trial

The scrambles used in all stimuli were composed from the set Ω comprising the nine grayscales with luminances $k\alpha$, for $k = 0, 1, \ldots, 8$ and $\alpha = 13.04\ \mathrm{cd/m^2}$. The homogeneous gray background had luminance $52\ \mathrm{cd/m^2}$ (equal to the fifth grayscale in Ω). We assume that the results reported here depend not on the actual luminances of grayscales but rather on their Weber contrasts relative to the gray field to which the participant is adapted: $-1.0, -0.75, \ldots, 1.0$.

Before and after each stimulus presentation, the participant viewed a homogeneous, mean-gray field. No chin rest was used. The participant fixated a small cue spot slightly brighter than the background and initiated a trial with a button-press. Following a 200 ms delay the stimulus was then presented for 167 ms. For some perturbation ρ, the stimulus comprised a target disk of scramble with histogram $U + \rho$ presented in one of eight locations in an annular background of scramble with histogram $U - \rho$. At the viewing distance of 85 cm, as indicated by Fig. 3, the target disk subtended 2.82° of visual angle and was centered in within the annulus 4.66° from fixation. The individual squares composing the scramble subtended 0.1° (i.e., 6′) of visual angle.

After the display, the participant used the number pad keys to indicate the location of the target disk. The mapping was: "7" for up-left, "8" for up, "9" for up-right, "6" for right, "3" for down-right, "2" for down, "1" for down-left, "4" for left. A beep sounded after any incorrect response.

2.5. Experimental conditions

Each participant performed 4500 trials in each of six, separately blocked conditions. Each of these conditions constitutes an individual application of the "seed expansion" method Chubb, Scofield, Chiao, and Sperling (2012). The next section gives a brief overview of the method as it applies in a single one of these six conditions in the current experiment.

2.5.1. The seed expansion method as used the current experiment

In a given separately blocked condition of the current experiment, a single dominant perturbation ϕ is used to define the difference between the target vs the background on each trial. The perturbation ϕ is called the *seed* of the condition. On any given trial in the condition with seed ϕ, the target will have a histogram $U + \rho$ for some perturbation ρ correlated strongly and positively with ϕ

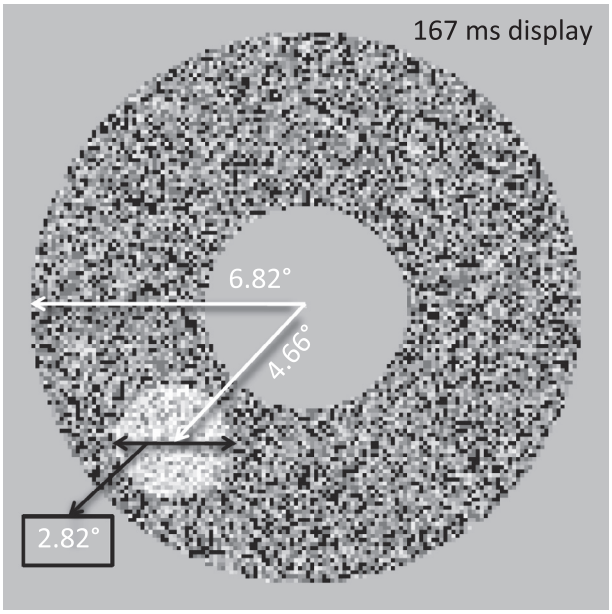

Fig. 3. *Stimulus dimensions and display duration.* On a given trial the participant fixated a small, central cue spot slightly brighter than the background and initiated a trial with a button-press. Following a 200 ms delay the stimulus was then presented for 167 ms. After the display, the participant used the number pad keys to indicate the location (up, up-right, right, down-right, down, down-left, left, or up-left) of the target disk. A beep sounded after any incorrect response.

(all correlations are 0.894 or higher), and the annular background will have histogram $U-\rho$. Thus, the qualitative difference between the target-disk vs the background will be similar from trial to trial. This feature of the design is intended to prompt the participant to use top-down attention to optimize his/her search strategy to exploit the constancy of this target-vs-background texture difference. In particular, we will assume that the participant combines information from his/her field-capture channels to produce a "grayscale filter" F_ϕ that gives high values to grayscales prevalent in the target and low values to grayscales prevalent in the background. It is by applying F_ϕ to the stimulus on a given trial that the participant is assumed to produce the search map in which the target location is signaled by heightened activation. By requiring that all perturbations ρ tested in the condition with the seed ϕ correlate strongly and positively with ϕ, we insure that the filter activation produced by the target on each trial will be greater than the filter activation produced by the background.

To characterize F_ϕ, we use a general linear model in which the regression variables are the values $\rho(\omega)$, for all $\omega \in \Omega$, and the linking function is a Weibull function. Specifically, we assume:

$$\Psi_\phi(\mathrm{Sal}_\phi(\rho)) = P_{chance} + (1 - P_{chance} - P_{finger})\left(1 - \exp\left(-\mathrm{Sal}_\phi(\rho)^{\beta_\phi}\right)\right). \quad (8)$$

where

1. $\mathrm{Sal}_\phi(\rho) = F_\phi \bullet \rho$ (9)

   is the "salience" of the target on a trial with perturbation ρ in the condition with seed ϕ,
2. $P_{chance} = 0.125$ (because the participant makes a forced choice from amongst 8 options), and
3. $P_{finger} = 0.02$ (to accommodate "finger errors," i.e., errors that participants might make even on trials in which they clearly discern the correct response).

In its usual formulation, the Weibull function has two parameters, a "steepness" parameter (β_ϕ in Eq. (8) and a "centering parameter" that usually appears as a denominator to the independent variable ($\mathrm{Sal}_\phi(\rho)$ in Eq. (8)). The reader will note that the centering parameter is missing from Eq. (8). This is because the centering parameter can be absorbed into the function F_ϕ in the expression $F_\phi \bullet \rho$ which is the argument to Ψ_ϕ in the context of this model.

Concerning Eq. (9): F_ϕ (in Eq. (9)) can be written as the sum of a function f_ϕ that sums to 0 plus an additive constant:

$$F_\phi(\omega) = f_\phi(\omega) + C_\phi. \quad (10)$$

Because any perturbation $\mathrm{Sal}_\phi(\rho)$ sums to 0, it follows that

$$\mathrm{Sal}_\phi(\rho) = F_\phi \bullet \rho = f_\phi \bullet \rho, \quad (11)$$

which shows that C_ϕ cannot be estimated. The function f_ϕ (the component of F_ϕ that *can* be estimated) is called the *expansion* of the seed perturbation ϕ.

2.5.2. The six seed conditions used in the current experiment

To describe the perturbations used in these experiments, we identify the 9 grayscales ranging from black to white in Ω with the corresponding Weber contrasts $v = -1, -0.75, \ldots, 1$. The Legendre polynomials of order $1, 2, \ldots, 8$ are listed in Table 1.[3] Our original reason (Chubb, Econopouly & Landy, 1994) for using the Legendre polynomials for this work was because they provided an easy way to isolate a space of scrambles all with the same mean and variance. In particular, for scrambles with histograms p and q,

1. if $p \bullet \lambda_1 = q \bullet \lambda_1$, then the two scrambles have the same mean grayscale, and
2. if in addition, $p \bullet \lambda_2 = q \bullet \lambda_2$, then they also have the same grayscale variance.

Thus, for any perturbation ρ derived by taking a linear combination of $\lambda_3, \lambda_4, \ldots, \lambda_8$, $(U+\rho)$-scramble has the same mean and variance as U-scramble.

The experiment comprised 6 different conditions corresponding to the seed perturbations $\phi = \lambda_1, -\lambda_1, \lambda_2, -\lambda_2, \lambda_3$, and $-\lambda_3$, examples of which are shown in Fig. 4. To make the difference in quality between target vs background as vivid as possible, these stimuli have the maximum possible histogram difference.

2.5.3. Trial-by-trial perturbations within a given seed condition

To allow the participant to use top-down attention to optimize his/her grayscale filter for seed perturbation ϕ, the perturbation used on each trial must correlate strongly and positively with ϕ. In addition, to enable efficient estimation of the expansion f_ϕ, the perturbations ρ tested across different trials should.

1. Have saliences yielding good but not perfect performance.
2. Span the space of all perturbations.
3. Probe dimensions in the space of perturbations orthogonal to ϕ in an evenhanded fashion.

We used the following method to satisfy these criteria in each of the six separately blocked seed conditions. The participant performed 4500 trials, 300 in each of 15 interleaved staircases, which we now define. Let $b_1 = \phi$, and let

$$b_2 = \begin{cases} \lambda_2 & \text{if } \phi = \pm\lambda_1 \\ \lambda_1 & \text{otherwise,} \end{cases} \quad (12)$$

and

$$b_3 = \begin{cases} \lambda_2 & \text{if } \phi = \pm\lambda_3 \\ \lambda_3 & \text{otherwise,} \end{cases} \quad (13)$$

and for $k = 4, 5, \ldots, 8$, let $b_k = \lambda_k$. Then for[4]

$$\epsilon_k = \begin{cases} 1/3 & \text{if } b_k = \lambda_1, \\ 1/2 & \text{otherwise,} \end{cases} \quad (14)$$

we construct the perturbations

$$\eta_k^+ = \frac{b_1 + \epsilon_k b_k}{\|b_1 + \epsilon_k b_k\|} \quad \text{and} \quad \eta_k^- = \frac{b_1 - \epsilon b_k}{\|b_1 - \epsilon b_k\|} \quad (15)$$

for $k = 2, 3, \ldots, 8$. Note that each of the perturbations $\rho = b_1$, as well as $\rho = \eta_k^+$ and $\rho = \eta_k^-$ for $k = 2, 3, \ldots, 8$, is normalized. Note also that if $\epsilon_k = \frac{1}{2}$ ($\epsilon_k = \frac{1}{3}$), then the correlation between ϕ and η_k is $\phi \bullet \eta_k = 0.8944$ ($\phi \bullet \eta_k = 0.9487$).

For each of the 15 perturbations $\rho = b_1, \eta_k^+, \eta_k^-, k = 2, 3, \ldots, 8$, psychometric data testing performance at localizing a target patch of $(U + A\rho)$-scramble in an annular background of $(U - A\rho)$-scramble was collected for various amplitudes A. Specifically, the

[3] The Legendre polynomials are derived by applying Gram–Schmidt orthonormalization to the sequence of monomials $h_j(v) = v^j, j = 0, 1, \ldots, 8$.

[4] The ϵ_k's need to strike a compromise. On the one hand, the higher the value of ϵ_k, the more power one has in estimating the contribution of λ_k to f_ϕ. On the other hand, if the perturbations away from ϕ are too large, then the assumption that Sal_ϕ is a linear function of the coordinate values of ρ (i.e., Eq. (9)) may fail. In particular, the high sensitivity of human vision to variations in λ_1 (which controls the difference between the mean Weber contrast of the target patch vs the background) leads us to restrict the contributions of λ_1 to the perturbations in the conditions with seeds $\pm\lambda_2$ and $\pm\lambda_3$ more tightly than the contributions of other non-seed λ_k's.

Table 1
The Legendre polynomials of order 1–8.

k	$\lambda_k(-1)$	$\lambda_k(-.75)$	$\lambda_k(-.5)$	$\lambda_k(-.25)$	$\lambda_k(0)$	$\lambda_k(.25)$	$\lambda_k(.5)$	$\lambda_k(.75)$	$\lambda_k(1)$
1	−0.5164	−0.3873	−0.2582	−0.1291	0.0000	0.1291	0.2582	0.3873	0.5164
2	0.5318	0.1330	−0.1519	−0.3229	−0.3799	−0.3229	−0.1519	0.1330	0.5318
3	−0.4449	0.2225	0.4132	0.2860	−0.0000	−0.2860	−0.4132	−0.2225	0.4449
4	0.3129	−0.4693	−0.2458	0.2011	0.4023	0.2011	−0.2458	−0.4693	0.3129
5	−0.1849	0.5085	−0.1849	−0.4160	0.0000	0.4160	0.1849	−0.5085	0.1849
6	0.0899	−0.3820	0.4944	0.0225	−0.4495	0.0225	0.4944	−0.3820	0.0899
7	−0.0341	0.2048	−0.4780	0.4780	−0.0000	−0.4780	0.4780	−0.2048	0.0341
8	0.0088	−0.0707	0.2473	−0.4942	0.6171	−0.4931	0.2462	−0.0703	0.0088

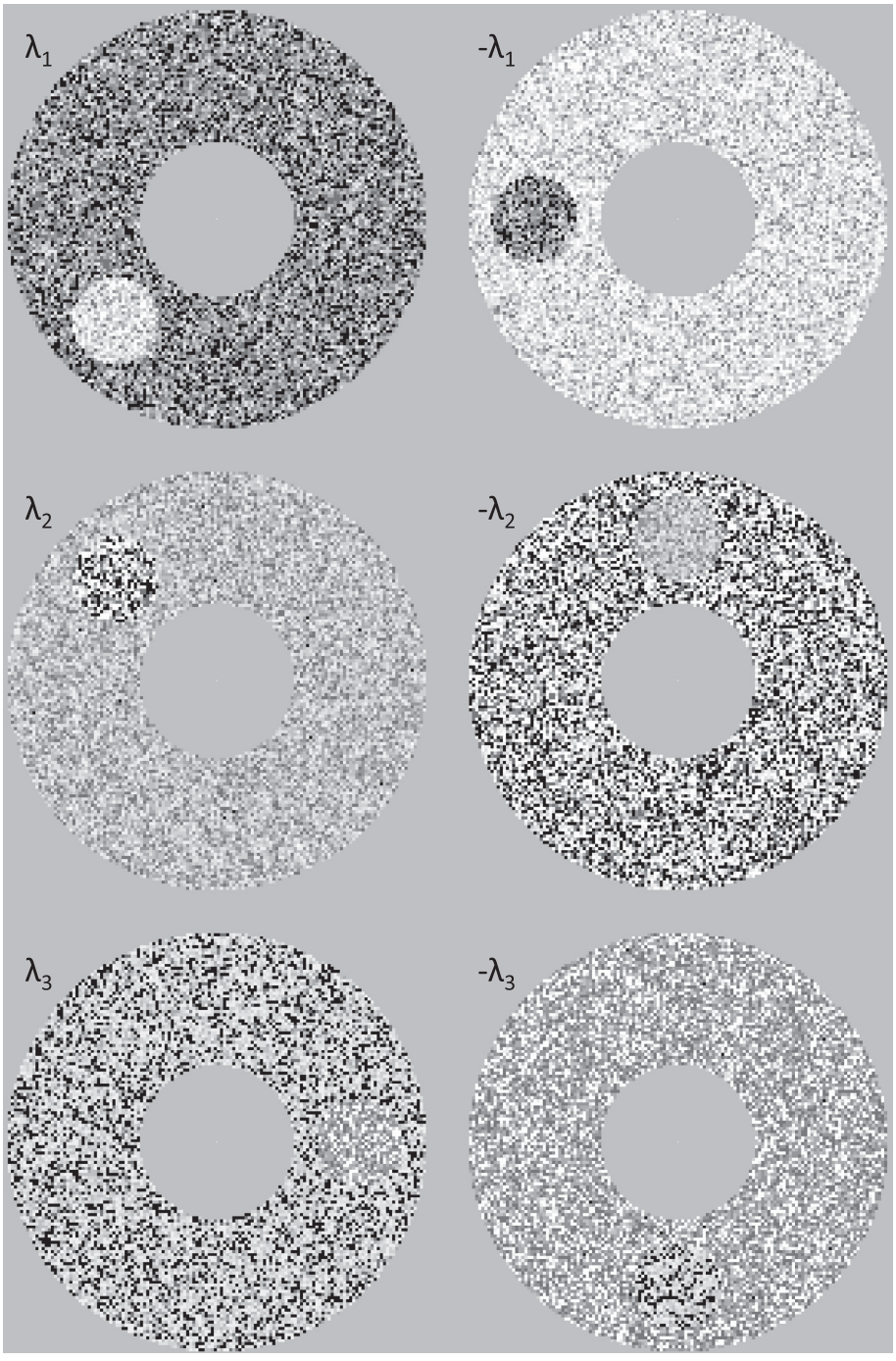

Fig. 4. *Stimulus conditions.* The target disks in the left-hand stimuli are composed of grayscale scramble with histogram $U + A_k\lambda_k$, for $k = 1$ (top), $k = 2$ (middle) and $k = 3$ (bottom), and the background annulus has histogram $U - A_k\lambda_k$, where the histogram amplitude A_k is chosen to make the perturbation $A_k\lambda_k$ maximal. The roles of target and background scramble are reversed in the stimuli on the right.

staircase for a given perturbation ρ could visit the 30 histogram amplitudes $A = \frac{A_{max}}{30}, \frac{2A_{max}}{30}, \ldots, A_{max}$, for A_{max} the scalar for which the maximum absolute value of $A_{max}\rho$ is equal to $\frac{1}{9}$. Each staircase started at amplitude $A = \frac{A_{max}}{2}$ and ran for 300 trials. In each staircase, A was decremented whenever the previous two trials both yielded correct responses; otherwise A was incremented. (Staircases that use this "2-down-1-up" update rule concentrate observations around perturbation amplitudes that yield performance in the neighborhood of 71% correct.) These 15 staircases (one for each of $\rho = b_1, \eta_k^+$ and $\eta_k^-, k = 2, 3, \ldots, 8$) were randomly interleaved to collect the 4500 trials of data in the condition with seed ϕ.

3. Results

3.1. Evidence of search asymmetries

In standard search tasks, one sometimes finds that search for a target of type *A* in a field of distractors of type *B* is more efficient than search for a target of type *B* in a field of distractors of type *A*. Such a result is called a "search asymmetry." For example, a search asymmetry holds between *c*'s and *o*'s (e.g., Treisman & Gormican, 1988): search for a *c* in a field of *o*'s is more efficient than search for an *o* in a field of *c*'s.

Search asymmetries place important constraints on theories of the field-capture channels resident in human vision. It is typically assumed that search for a target of type *A* amongst a field of distractors of type *B* is efficient only if there exists in human vision one or more field-capture channels that are activated by objects of type *A* but not by objects of type *B*. Thus, for example, the finding that search is easy for a *c* amongst *o*'s implies that human vision has a field-capture channel that is activated by *c*'s but not by *o*'s; conversely, the finding that search is hard for an *o* amongst *c*'s implies that all field-capture channels activated by *o*'s are also activated by *c*'s.

In the current context, a search asymmetry is said to hold for a given seed perturbation ϕ and a given participant j if $f_{j,\phi} \neq -f_{j,-\phi}$ (i.e., if the expansions $f_{j,\phi}$ and $f_{j,-\phi}$ derived for participant j from complementary task conditions fail to be negatives of each other).

The expansions estimated from our six different seed conditions are plotted in Fig. 5 so as to reveal whatever search asymmetries exist. Each row of three panels presents the results for one participant for $\phi = \lambda_1, \lambda_2$ and λ_3 (from left to right). The dim dashed line in each panel shows ϕ. The white curve shows the expansion $f_{j,\phi}$ derived for participant $j = 1, 2, 3$ from the condition with seed ϕ; the black curve shows $-f_{j,-\phi}$, the negative of the expansion derived for participant j from the condition with seed $-\phi$. A search asymmetry exists if the white and black curves differ in form. Error bars are 95% Bayesian credible intervals. Note that the search asymmetries are especially striking for $\phi = \lambda_3$. Likelihood ratio tests of the null hypothesis that $f_{j,\phi} = -f_{j,-\phi}$ yield vanishingly small p-values for the results in all 9 panels of Fig. 5 except in the case of $\phi = \lambda_2$ for *S*1, for which $\chi^2_{df=8} = 18.88, p = 0.016$.

3.2. Preliminary model

A preliminary model was applied to the data from all six seed conditions separately for each of the three participants. This model assumed that:

1. The participant has some number N_{FCCs} of field-capture channels with modulators f_k for $k = 1, 2, \ldots, N_{FCCs}$.
2. For any given seed ϕ, the expansion f_ϕ is the (unique) weighted sum

$$f_\phi = \sum_{k=1}^{N_{FCCs}} w_{\phi,k} f_k \tag{16}$$

for which the weights $w_{\phi,1}, w_{\phi,2}, \ldots, w_{\phi,N_{FCCs}}$ are chosen to maximize $f_\phi \bullet \phi$ under the constraints that they are all nonnegative and sum to 1.

3. On a trial with perturbation ρ in the condition with seed ϕ,
   (a) the salience of target is

$$\mathrm{Sal}_\phi(\rho) = f_\phi \bullet \rho, \tag{17}$$

   (b) and, for $P_{chance} = 0.125$ and $P_{finger} = 0.02$, the probability of a correct response is

$$\Psi(\mathrm{Sal}_\phi(\rho)) = P_{chance} + (1 - P_{chance} - P_{finger})\left(1 - \exp\left[-\mathrm{Sal}_\phi(\rho)^\beta\right]\right) \tag{18}$$

(Note the implicit assumption that the Weibull steepness parameter β is fixed across different seed conditions.)

3.2.1. Results from the preliminary model

1. For all three participants, N_{FCCs} had to be at least 4 to obtain reasonable fits.
2. The predicted sensitivity function modulators f_1, f_2, f_3 and f_4 were qualitatively similar for all three participants. These included
   (a) a modulator qualitatively similar to the blackshot sensitivity function,
   (b) a modulator whose sensitivity is minimal for black, rises sharply to its maximum for grayscales slightly darker than mid-gray, then falls to uniform half-height for all higher grayscales,
   (c) a modulator whose sensitivity is minimal for black, increases linearly with increasing grayscale and reaches its maximum near white,
   (d) a modulator (complementary to channel 2c) whose sensitivity is maximal for black decreases linearly and reaches its minimum near white.

Especially striking was the result that these modulators (c) and (d) were close to negatives of each other for all three participants.

3.3. The 3-dimensional, 4-channel (3D4C) model

The preliminary analyses described in Section 3.2 suggested that it might be possible to derive an adequate description of the results using a model that fit the data from all three participants across all six conditions under the following assumptions:

1. Human vision has four field-capture channels sensitive to gray-scale scrambles whose normalized modulators f_1, f_2, f_3, and f_4 satisfy the constraint that $f_4 = -f_3$.
2. All participants share these same four field-capture channels; however, participants may vary in their relative sensitivity to information from these different channels. Thus, for participants $j = 1, 2, 3$, the modulators of field-capture channels $k = 1, 2, 3, 4$ are $f_{j,k} = A_{j,k} f_k$ for nonnegative amplitudes $A_{j,k}$ reflecting the sensitivities of different participants j to information from different field-capture channels k.
3. For a given seed perturbation ϕ, the expansion $f_{j,\phi}$ achieved by participant $j = 1, 2, 3$ is the weighted sum

$$f_{j,\phi} = \sum_{k=1}^{4} w_{j,k} f_{j,k} \tag{19}$$

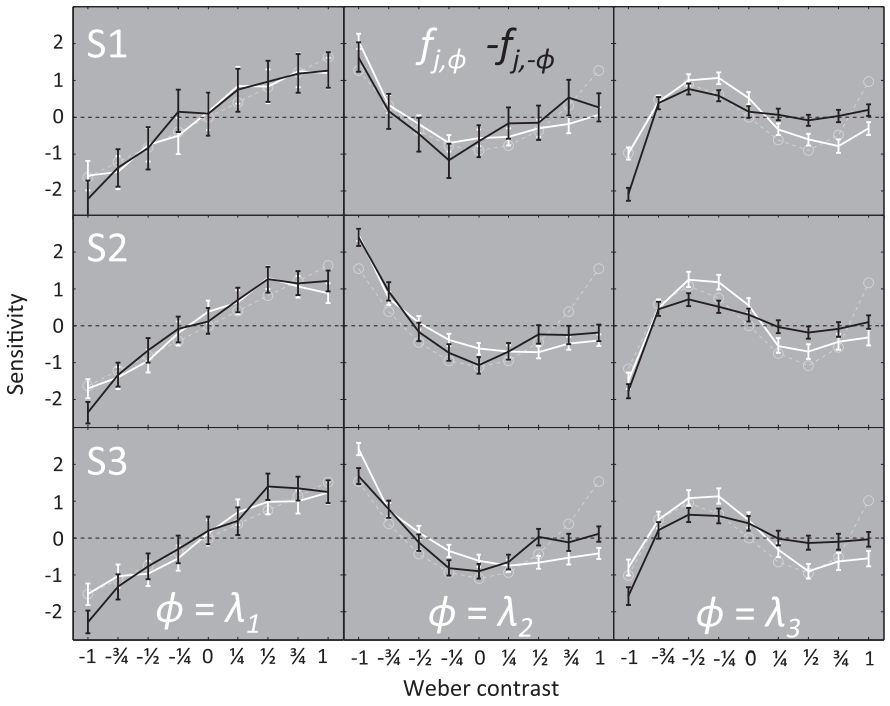

Fig. 5. *Search Asymmetries.* Each row of three panels presents the results for one participant for $\phi = \lambda_1, \lambda_2$ and λ_3 (from left to right). The dim dashed line in each panel shows ϕ. The white curve shows the expansion $f_{j,\phi}$ derived for participant *Sj* ($j = 1,2,3$) from the condition with seed ϕ; the black curve shows $-f_{j,-\phi}$, the negative of the expansion derived from the condition with seed $-\phi$. A search asymmetry exists if the white and black curves differ in form. Error bars are 95% Bayesian credible intervals. Note that the search asymmetries are especially striking for $\phi = \lambda_3$.

in which the weights are chosen optimally for the task at hand: that is, the weights are chosen to maximize $f_{j,\phi} \bullet \phi$ under the constraint that $w_{j,1}, w_{j,2}, w_{j,3}$, and $w_{j,4}$ are nonnegative and sum to 1. Thus,

4. For participant $j = 1,2,3$, on a trial in which the target is defined by perturbation ρ in the condition with seed ϕ,
   (a) the salience of target is

$$\mathrm{Sal}_{j,\phi}(\rho) = f_{j,\phi} \bullet \rho, \tag{20}$$

   (b) and for $P_{chance} = 0.125$ and $P_{finger} = 0.02$, the probability of a correct response is

$$\Psi_j(Sal_{j,\phi}(\rho)) = P_{chance} + (1 - P_{chance} - P_{finger})\left(1 - \exp\left[-\mathrm{Sal}_{j,\phi}(\rho)^{\beta_j}\right]\right). \tag{21}$$

(Note the assumption that the Weibull exponent β_j may differ for different participants $j = 1,2,3$; however, for participant j, β_j is fixed across different seed conditions.)

Each of the normalized field-capture channel modulators f_k is constrained to sum to 0 and to satisfy $\|f_k\| = 1$; thus, these functions collectively contribute $3 \times (9 - 2) = 21$ degrees of freedom. f_4 is determined by f_3, so it adds no degrees of freedom. Each of the parameters β_j and $A_{j,k}, j = 1,2,3, k = 1,2,3,4$ adds a degree of freedom, yielding 15 additional degrees of freedom. The $w_{j,k}$'s occurring in Eq. (19) are completely determined by the constraints they are required to satisfy; hence, they contribute no degrees of freedom. Thus the total number of degrees of freedom in the 3D4C model is 36.

3.4. Results of fitting the 3D4C model

The left panel in Fig. 6 shows the four estimated field-capture channel sensitivity functions $F_{1,k}(\omega), k = 1,2,3,4$, for participant *S*1, and the center and right panels show the corresponding results for participants *S*2 and *S*3. Only the field-capture channel modulators $f_{j,k} = A_{j,k} f_k(\omega)$ have actually been estimated from the model fit; we have taken the liberty of setting the field-capture channel baseline constant $C_{j,k} = -\min\{f_{j,k}\}$ in each case to make $\min\{F_{j,k}\} = 0$. The sensitivity functions $F_{j,1}$ show the sharp tuning to black characteristic of the blackshot sensitivity function. Sensitivity functions $F_{j,2}$ characterize a previously unknown field-capture channel selective for midrange grays slightly darker than the mean. The sensitivity function $F_{j,3}$ ($F_{j,4}$) shows linearly increasing (decreasing) sensitivity to grayscale across the gamut, reaching its maximum (minimum) near the high end.

Fig. 7 plots the expansions predicted by the 3D4C model for all three participants juxtaposed with the expansions estimated individually from the data for the different seed conditions. The number of degrees of freedom used to produce the black (white) curves in Fig. 7 is $9 \times 3 \times 6 = 162$ (36). However, the white curves account for more than 98% of the variance in the trial-by-trial saliences (across all 81,000 trials) predicted using the expansions (the black curves) estimated separately for all participants in all seed conditions.

3.5. Model comparisons

The 3D4C model is tightly sandwiched in a nested sequence between two models. The more general model is the "4-channel" (4C) model in which the normalized modulator of the fourth channel is not required to satisfy $f_4 = -f_3$. The more restricted model is the "2-unsigned channel, 1-signed channel" (2U1S) model which imposes the additional constraint that

$$A_{j,4} = A_{j,3} \text{ for participants } \quad j = 1,2,3. \tag{22}$$

Note that if Eq. (22) is satisfied, then $f_{j,4} = A_{j,4} f_4 = -A_{j,3} f_3 = -f_{j,3}$, implying that the term $w_{j,4} f_{j,4}$ occurring in Eq. (19) can be written as $-w_{j,4} f_{j,3}$ which in turn implies that Eq. (19) can be written

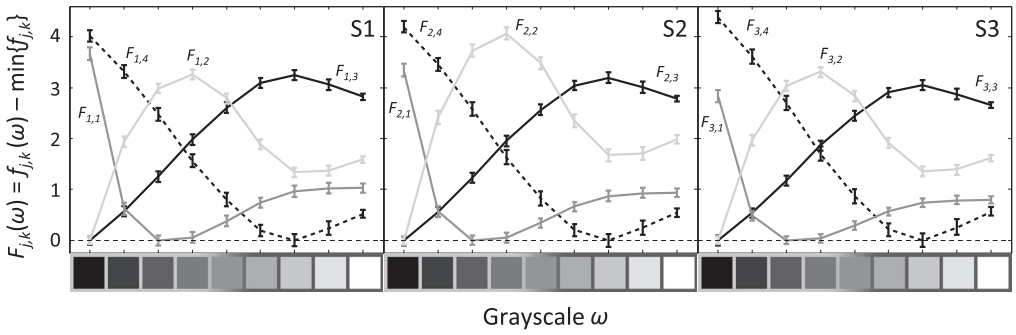

Fig. 6. *Estimated field-capture channel sensitivity functions.* Fitting the 3D4C model jointly to the data for all three participants j = 1,2,3 yields the 12 estimated field-capture channel sensitivity functions $F_{j,k}(\omega) = C_{j,k} + f_{j,k}(\omega)$. In each case, the sensitivity modulator $f_{j,k}$ has been estimated from the model fit, and the baseline constant $C_{j,k}$ has been set to $-\min\{f_{j,k}\}$ to make the minimum value of $F_{j,k}$ equal to 0. Results are shown for participants S1, S2 and S3 in the three panels from left to right. Note that sensitivity functions $F_{j,1}$ (j = 1,2,3) closely resemble the blackshot sensitivity function. Sensitivity functions $F_{j,2}$ characterize a previously unknown field-capture channel selective for midrange grays slightly darker than the mean. Sensitivity functions $F_{j,3}$ and $F_{j,4}$ are linearly dependent; specifically, for a given participant j, modulator $f_{j,4} = -\alpha_k f_{j,3}$ for $\alpha_k > 0$. The sensitivity function $F_{j,3}$ ($F_{j,4}$) shows linearly increasing (decreasing) sensitivity to grayscale across the gamut, reaching its maximum (minimum) near the high end. Error bars are 95% Bayesian credible intervals.

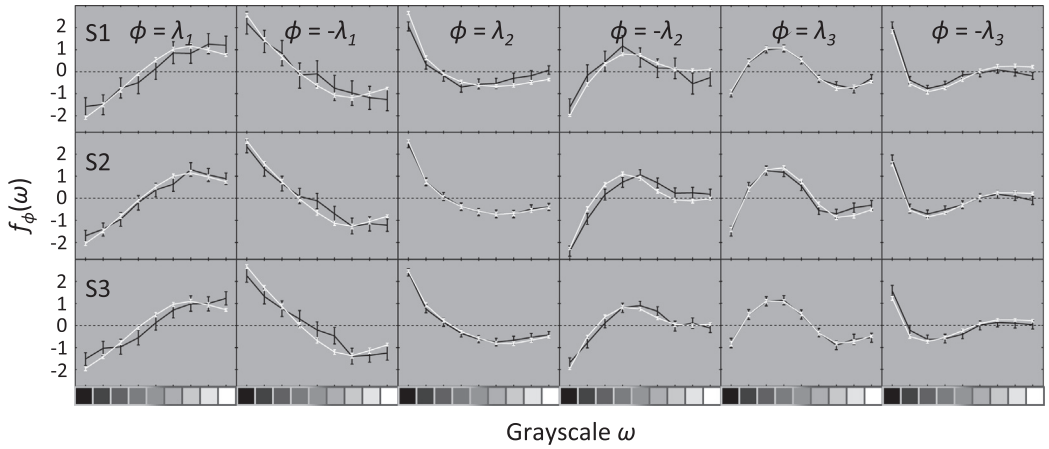

Fig. 7. *Expansions predicted by the 3D4C model.* Expansions estimated from the 3D4C model (plotted in white) and expansions estimated from the data from individual seed conditions (plotted in black) for each of the three participants. Error bars are 95% Bayesian credible intervals. Note that the 3D4C model expansions (white curves-based on 39 degrees of freedom) account for more than 98% of the variance in the trial-by-trial saliences (across all 81,000 trials) estimated using the expansions (the black curves) derived separately for all participants in all seed conditions.

$$f_{j,\phi} = \sum_{k=1}^{3} w_{j,k} f_{j,k} \tag{23}$$

where the sign of $w_{j,3}$ is the same as that of $f_3 \bullet \phi$. Thus, the additional constraint imposed by Eq. (22) leads to a model with only three field-capture channels, the third of which produces signed responses; this allows the coefficient $w_{j,3}$ to vary in sign in Eq. (23).

Likelihood ratio tests were used to compare the 3D4C model with each of the 2U1S and 4C models. The likelihood ratio test (e.g., Hoel, Port & Stone, 1971) compares the maximum likelihood $\widehat{\Lambda}_{restricted}$ of the more restricted model to the maximum likelihood $\widehat{\Lambda}_{fuller}$ of the more general model. As shown by Wilks (1938), if the restricted model captures the true state of the world, then the statistic $-2\ln(\widehat{\Lambda}_{restricted}/\widehat{\Lambda}_{fuller})$ is asymptotically distributed as $\chi^2_{(v)}$ where the number of degrees of freedom v is equal to the number of free parameters in the unconstrained model minus the number of free parameters in the constrained model. The test in which the restricted model was the 2U1S model and the fuller model was the 3D4C model yielded $\chi^2_{(3)} = 341.27$ (p infinitesimal), emphatically rejecting the null hypothesis that the 2U1S model captures the true state of the world. On the other hand, the test in which the restricted model was the 3D4C model and the fuller model was the 4C model yielded $\chi^2_{(7)} = 2.97$ ($p = 0.887$) lending striking support to claim that field-capture channels 3 and 4 do indeed have complementary modulators.

4. Discussion

4.1. Implications of search asymmetries

A single important conclusion follows immediately from the search asymmetries documented in Fig. 5. Previous investigations of grayscale scramble discrimination (Chubb, Econopouly & Landy, 1994; Chubb, Landy & Econopouly, 2004; Chubb et al., 2007) have assumed (by analogy to color perception) that

1. The visual impact of a scramble can be summarized by the vector of activations the scramble produces in scramble-selective field-capture channels.
2. The salience of the difference between two scrambles is a Minkowski distance between the vectors of activations they produce.
3. The probability of a correct response in a task requiring discrimination of two scrambles is a psychometric function of the salience of the difference between them.

However, by definition, any distance $D(v,w)$ between vectors v and w satisfies $D(v,w) = D(v,w)$; that is, the distance of v from w is equal to the distance of w from v. In the current context, assumption 2. above implies that the salience of a target disk of $(U+\phi)$-scramble in a background of $(U-\phi)$-scramble should be equal to

the salience of a target patch of $(U-\phi)$-scramble in a background of $(U+\phi)$-scramble which in turn implies that the task of detecting a patch of $(U+\phi)$-scramble in a background of $(U-\phi)$-scramble should yield performance identical to the task of detecting a patch of $(U-\phi)$-scramble in a background of $(U+\phi)$-scramble. The search asymmetries observed in the current experiment contradict this prediction.

The 3D4C model assumes that in the condition with seed ϕ, the participant uses top-down attentional control to linearly combine the responses of his/her field-capture channels to synthesize a "grayscale filter" that is optimal for detecting a patch of $(U+\phi)$-scramble in a background of $(U-\phi)$-scramble. Importantly, the optimal filter for the complementary task is likely to be different. The 3D4C model proposes that the search asymmetries evident in Fig. 5 reflect differences of this sort in the grayscale filters deployed in complementary seed conditions.

4.2. The 3D4C model assumptions: How plausible are they?

We acknowledge that the 3D4C model makes several very strong assumptions that are unlikely to be strictly true; these include the following:

1. The field-capture channels of different participants have sensitivity functions whose modulators are identical except for different scale factors.
2. Participants can take arbitrary linear combinations of field-capture channel responses to construct the grayscale filters they use in different seed conditions.
3. In producing the grayscale filters they use in particular seed conditions, participants always combine the responses of their field-capture channels with weights that are optimal for the current seed condition.

Despite these implausibly strong assumptions, however, the 3D4C model provides a remarkably clean summary of the substantial body of data provided by three participants across six different seed conditions in this study. Indeed, the success of the model provides support for the claim that the strong assumptions upon which it is founded may in fact hold reasonably well.

It should also be noted that the 3D4C model is consistent with previous findings. First, the finding that the modulators of the field-capture channel sensitivity functions span a 3-dimensional space is consistent with previous results Chubb et al. (2007). Second, the 3D4C model imposes no constraints upon the normalized modulators f_1, f_2, and f_3 used to generate the four field-capture channel sensitivity functions of all three participants; nonetheless, the normalized modulator f_1 (used to generate $F_{j,1}$ in Fig. 6 for each participant $j = 1, 2, 3$) closely resembles the sensitivity function of the blackshot field-capture channel implicated by previous experiments Chubb, Econopouly and Landy (1994) and Chubb, Landy and Econopouly (2004).

The 3D4C model thus emerges as a theory of how human observers process grayscale scrambles. Of central interest is the finding that human vision includes four field-capture channels whose sensitivity functions conform to those shown in each of the panels in Fig. 6 (up to the unmeasured baseline constants that have been set to $-\min\{f_{j,k}\}$ in Fig. 6).

Let us call these 4 channels.

1. the *blackshot* channel (characterized by sensitivity function $F_{j,1}$ for participant $j = 1, 2, 3$ in Fig. 6),
2. the *gray-tuned* channel (characterized by sensitivity function $F_{j,2}$),
3. the *up-ramped* channel (characterized by sensitivity function $F_{j,3}$),
4. the *down-ramped* channel (characterized by sensitivity function $F_{j,4}$),

bearing in mind that the normalized modulators f_3 and f_4 of the up-ramped and down-ramped channels are required by the 3D4C model to satisfy $f_4 = -f_3$.

4.3. The relation between the 3D4C model and the ON- and OFF-systems

A substantial body of research suggests that human vision is asymmetric in its processing of negative vs positive contrast polarities, with negative contrast polarities processed faster and more efficiently than positive polarities (Blackwell, 1946; Bowen, Pokorny & Smith, 1989; Chan & Tyler, 1992; Chubb, Econopouly & Landy, 1994; Chubb, Landy & Econopouly, 2004; Chubb & Nam, 2000; Dannemiller & Stephens, 2001; Jin, Wang, Lashgari, Swadlow, & Alonso, 2011; Komban, Alonso & Zaidi, 2011; Konstevich & Tyler, 1999; Krauskopf, 1980; Lu & Sperling, 2012; Short, 1966; Whittle, 1986; Xing, Yeh & Shapley, 2010; Yeh, Xing & Shapley, 2009). The results of most of the previous studies can be understood in terms of two processes, an ON-system process whose response is zero for negative Weber contrasts and increases in a smoothly graded fashion as a function of positive Weber contrast, and a corresponding OFF-system process whose response is zero for positive Weber contrasts and increases in a smoothly graded fashion as a function of increasingly negative Weber contrasts. Asymmetries in the processing of negative vs positive Weber contrasts have usually been ascribed to differences in the computations performed by the ON- vs OFF-systems.[5]

One might construe the down-ramped sensitivity function as the response function of the OFF-system. However, the down-ramped function decreases continuously across Weber contrasts from -1 up to 0.75. This range seems too broad to reflect the OFF-system in isolation. Even more striking, not one of the field-capture channels posited by the 3D4C model has a sensitivity function that bears any resemblance at all to the response function of the ON-system. This raises the question: what is the relation between the four field-capture channels posited by the 3D4C model and the ON- and OFF-systems?

4.3.1. Hypothesis: the up- and down-ramped channels are differences of ON- and OFF-responses

We hypothesize that each of the up-ramped and down-ramped field-capture channels is derived by combining the responses of the ON- and OFF-systems in push–pull fashion; specifically:

1. The functions that characterize the responses of the OFF- and ON-systems to grayscale scrambles are f_{OFF} and f_{ON} plotted in Fig. 8.
2. The up-ramped field-capture channel is derived by taking

$$f_{\text{up-ramped}}(\omega) = A_{\text{up}}\left(f_{ON}(\omega) - f_{OFF}(\omega) + C_{\text{up}}\right) \quad \text{for all } \omega \in \Omega \tag{24}$$

for positive scalars A_{up} and $C_{\text{up}} > \max\{f_{OFF}\}$.

3. The down-ramped field-capture channel is derived by taking

$$f_{\text{down-ramped}}(\omega) = A_{\text{down}}\left(f_{OFF}(\omega) - f_{ON}(\omega) + C_{\text{down}}\right) \quad \text{for all } \omega \in \Omega \tag{25}$$

for positive scalars A_{down} and $C_{down} > \max\{f_{ON}\}$.

[5] Exceptions include Whittle (1986), Chubb, Econopouly and Landy (1994) and Chubb, Landy and Econopouly (2004) which implicate a visual process that is most naturally viewed as tuned to Weber contrasts very near -1, with a response that drops rapidly to 0 with increasing Weber contrasts (i.e., for Weber contrasts greater than around -0.9).

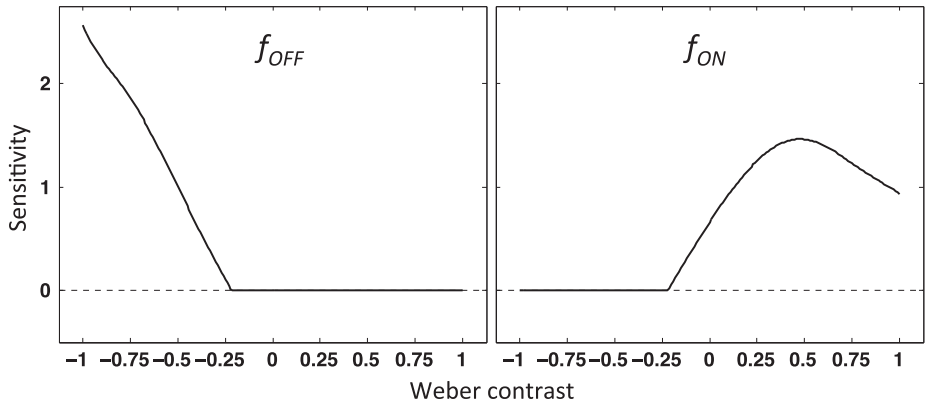

Fig. 8. *Hypothetical OFF- and ON-system response functions.* Suppose the functions characterizing the responses of the OFF- and ON-systems to grayscale scrambles are given by f_{OFF} and f_{ON}. In this case, the up-ramped (down-ramped) field-capture channel can be derived by combining f_{Off} and f_{ON} as in Eq. (24) (Eq. (25)).

The reader will note that f_{ON} and f_{OFF} do not hit the Weber contrast axis at 0 as might be expected. This is hardly surprising, however, given that

1. each of the texture elements in a grayscale scramble occurs in a dense, highly variable context that is likely to include both dark and bright abutting elements, and
2. the dark elements plausibly exert greater influence in determining the effective zero for each of the ON- and OFF-system responses (Blackwell, 1946; Bowen, Pokorny & Smith, 1989; Chan & Tyler, 1992; Chubb, Econopouly & Landy, 1994; Chubb, Landy & Econopouly, 2004; Chubb & Nam, 2000; Dannemiller & Stephens, 2001; Jin et al., 2011; Komban, Alonso & Zaidi, 2011; Konstevich & Tyler, 1999; Krauskopf, 1980; Lu & Sperling, 2012; Short, 1966; Whittle, 1986; Xing, Yeh & Shapley, 2010; Yeh, Xing & Shapley, 2009).

The reader will also note that f_{ON} is nonmonotonic with increasing Weber contrast. Although this might seem surprising, it should be noted that a similar nonmonotonicity has previously been observed an experiment in which participants strove to judge which of two grayscale scrambles had higher mean grayscale (Nam & Chubb, 2000). Indeed the sensitivity functions derived in that study were similar in form to $f_{\text{up-ramped}}$ plotted in Fig. 6.

4.4. The blackshot and gray-tuned field-capture channels

A field-capture channel sharply tuned to very black elements in the visual input has been implicated in several previous studies (Chubb, Econopouly & Landy, 1994; Chubb, Landy & Econopouly, 2004; Whittle, 1986); thus, the fact that this "blackshot" channel falls out of the analysis as one of the four field-capture channels in the 3D4C model solidifies confidence in the model. It is natural to assume that the blackshot field-capture channel is distilled from the OFF-system response, and there is evidence to suggest that the extraction of the blackshot signal may require integration of information over time. In his classic study of luminance increment and decrement thresholds (Whittle, 1986), Whittle discovered that observers were exquisitely sensitive to small differences between luminances very close to black, even though the targets to be discriminated were presented against a background of photopic luminance. Whittle also noted that the system mediating performance in this task was fairly slow, requiring around 250 ms to reach peak sensitivity. Consonant with this observation, the experiments that first measured the blackshot sensitivity function used displays of 250 ms Chubb, Econopouly and Landy (1994) and 200 ms Chubb, Landy and Econopouly (2004). With that said, however, very little is known about the blackshot field-capture channel. In particular, nothing is known either about the process by which the blackshot signal is extracted or about the neural substrate of the blackshot channel.

The gray-tuned field-capture channel has not been previously documented, and we have no good account to offer of its relation to the ON- and OFF-systems. Several observations seem potentially useful, however:

1. The steepness of the gray-tuned channel sensitivity function near Weber contrast −1.0 suggests that the gray-tuned channel may depend on some of the same processes as the blackshot channel. Indeed, the gray-tuned channel sensitivity function bears some resemblance to the negative of the blackshot sensitivity function.
2. The peak sensitivity of the gray-tuned channel is to Weber contrasts near −0.25. This is also the Weber contrast hypothesized to produce activation 0 in each of the ON- and OFF-systems in the context of a grayscale scramble. Under this hypothesis, then, the gray-tuned channel is maximally activated by Weber contrasts that produce minimal activation in the ON- and OFF-systems.

5. Summary

Each of three participants performed 4500 trials in each of six different conditions of a task requiring him/her to detect the location of a patch of grayscale scramble in a background of different scramble. In a given condition, the quality that differentiated the target from the background was kept approximately constant from trial to trial to enable the participant to optimize a grayscale filter for the condition. Preliminary analysis of the data from individual participants suggested that a model might be fit (to the 81,000 trials of data from all three participants across all six conditions) that was based on the following assumptions:

1. Human vision has four field-capture channels that are differentially sensitive to grayscale scrambles.
2. Two of these field-capture channels have sensitivity functions whose normalized deviations from their means are negatives of each other.
3. Different participants share these same four field-capture channels but may differ in their sensitivity to information from the four channels.
4. In performing tasks of the sort required in the current experiments, participants can produce grayscale filters by taking linear combinations of the outputs from their four field-capture channels. Moreover,

5. In a given task condition in the current experiment, a given participant always uses the particular linear combination of field-capture channels (with nonnegative weights that sum to 1) that is optimal for the task variant tested in that condition.

The model itself leaves the forms of three of the field-capture sensitivity functions unconstrained while constraining the fourth to mirror the third in the sense of assumption 2 above.

The resulting fit accounted for more than 98% of the variance in the trial-by-trial salience observed in the results from individual task conditions. The four field-capture channels predicted by the model were:

1. the *blackshot* channel (characterized by sensitivity function $F_{j,1}$ for participant $j = 1, 2, 3$ in Fig. 6),
2. the *gray-tuned* channel (characterized by sensitivity function $F_{j,2}$),
3. the *up-ramped* channel (characterized by sensitivity function $F_{j,3}$),
4. the *down-ramped* channel (characterized by sensitivity function $F_{j,4}$), with the down-ramped sensitivity function constrained to mirror the up-ramped sensitivity function.

Because these four field-capture channels collectively confer sensitivity to a 3-dimensional space of histogram variations, the model is called the 3D4C model.

Acknowledgments

We are grateful to George Sperling and Ted Wright for helpful insights. This work was supported by NSF Award BCS-0843897.

Appendix A

This appendix describes the details of the Bayesian model-fitting methods used in this paper. The paper derives estimates of parameters from two different models:

1. the basic seed-expansion model captured by Eqs. (9) and (8) in Section 2.5.1,
2. the 3D4C model described in Section 3.3.

In each case, Markov chain Monte Carlo simulation was used to estimate the joint posterior density characterizing model parameters. To derive the sample from the posterior joint density, the algorithm needs to iteratively evaluate the model likelihood function.

A.1. The likelihood function used to fit the basic seed expansion model

The model used to estimate the expansion f_ϕ achieved by given participant in the condition with seed perturbation ϕ has parameters $\beta_\phi \in \mathbb{R}^+$ and $f_\phi : \Omega \to \mathbb{R}$ that sums to 0.

The likelihood function for this model is defined as follows for any $\beta \in \mathbb{R}^+$ and any $f : \Omega \to \mathbb{R}$ that sums to 0:

$$\Lambda_{\text{Basic},\phi}(f,\beta) = \prod P_\phi(t \mid f,\beta)^{c_\phi(t)}(1 - P_\phi(t \mid f,\beta))^{(1-c_\phi(t))} \tag{26}$$

where

1. the product is over all trials t performed by the participant in the condition with seed perturbation ϕ,
2. $c_\phi(t) = 1$ if the response on trial t is correct and 0 if incorrect,
3. and the probability $P_\phi(t \mid f,\beta)$ that the participant responds correctly on the t^{th} trial in the condition with seed ϕ under the assumption that $f_\phi = f$ and $\beta_\phi = \beta$ is given by

$$P_\phi(t \mid f,\beta) = P_{chance} + (1 - P_{chance} - P_{finger}) \times \left(1 - \exp\left[-(f \bullet \rho_{\phi,t})^\beta\right]\right) \tag{27}$$

for $P_{chance} = 0.125, P_{finger} = 0.02$, and $\rho_{\phi,t}$ the perturbation used to generate the stimulus on the t^{th} trial for the participant in the condition with seed ϕ.

A.2. The likelihood function used to fit the 3D4C model

Let

1. $\rho_{t,j,\phi}$ be the perturbation used to define the target scramble presented to participant j on trial t of the condition with seed ϕ, and
2. $c(t,j,\phi) = 1$ if the participant responded correctly on this trial or $c(t,j,\phi) = 0$ if incorrectly.

The parameters of the 3D4C model are functions $f_k : \Omega \to \mathbb{R}, k = 1, 2, 3$, each of which sums to 0 and satisfies $\|f_k\| = 1$, nonnegative Weibull function exponents β_j and nonnegative sensitivity function amplitudes $A_{j,k}$ for participants $j = 1, 2, 3$ and field-capture channels $k = 1, 2, 3, 4$. The likelihood function for the 3D4C model is defined as follows for any η comprising guesses at these 42 parameters (with 36 degrees of freedom):

$$\Lambda_{3D4C}(\eta) = \prod P(t,j,\phi \mid \eta)^{c(t,j,\phi)}(1 - P(t,j,\phi \mid \eta))^{(1-c(t,j,\phi))} \tag{28}$$

where, for $P_{chance} = 0.125$ and $P_{finger} = 0.02$, the probability (given η) that participant j responds correctly on trial t in the condition with seed ϕ is

$$P(t,j,\phi \mid \eta) = P_{chance} + (1 - P_{chance} - P_{finger})\left(1 - \exp\left[-(f_{j,\phi} \bullet \rho_{t,j,\phi})^{\beta_j}\right]\right) \tag{29}$$

and the expansion $f_{j,\phi}$ achieved by participant j in the condition with seed ϕ is

$$f_{j,\phi} = w_{j,\phi,1} f_{j,1} + w_{j,\phi,2} f_{j,2} + w_{j,\phi,3} f_{j,3} + w_{j,\phi,4} f_{j,4} \tag{30}$$

where

1. the modulators of participant j's field-capture channel sensitivity functions are

$$f_{j,k} = A_{j,k} f_k, \quad \text{and} \quad f_{j,4} = -A_{j,4} f_3 \quad \text{for} \quad k = 1, 2, 3, \tag{31}$$

and

2. the vector of weights $w_{j,\phi} = (w_{j,\phi,1}, w_{j,\phi,2}, w_{j,\phi,3}, w_{j,\phi,4})$ is chosen to maximize $f_{j,\phi} \bullet \phi$ under the constraints that

$$\sum_{k=1}^{4} w_{j,\phi,k} = 1 \quad \text{and} \quad w_{j,\phi,k} \geqslant 0 \quad \text{for} \quad k = 1, 2, 3, 4. \tag{32}$$

As is easily shown, this condition is achieved by setting

$$w_{j,\phi} = \frac{\tilde{w}_{j,\phi}}{\sum_{k=1}^{4} \tilde{w}_{j,\phi,k}} \tag{33}$$

for

$$\tilde{w}_{j,\phi,k} = \max\{0, f_{j,k} \bullet \phi\}, \quad k = 1, 2, \ldots, 4. \tag{34}$$

A.2.1. Markov chain Monte Carlo simulation

The estimation method uses Markov chain Monte Carlo (MCMC) simulation. For simplicity, uniform prior distributions are used for all parameters. In any MCMC process using uniform priors, one starts with some arbitrary guess at the parameter vector V (which will ultimately be thrown away) and sets ${}_1S = V$; then one iterates the following steps some large number N of times. (Pre-subscripts will be used to indicate sample number in the MCMC process and

ordinary subscripts to indicate the coordinate within a given sample.) In the current application of this method, V comprises guesses at the model parameters. Then[6]

for

$$ {}_nR = \frac{\Lambda(C)}{\Lambda({}_{n-1}S)} \tag{35} $$

- if ${}_nR \geqslant 1$, set ${}_nS = C$;
- otherwise set

$$ {}_nS = \begin{cases} C & \text{with probability } {}_nR \\ {}_{n-1}S & \text{with probability } 1 - {}_nR \end{cases}. \tag{36} $$

In practice, to keep the computation within range of floating point representation, one never actually computes $\Lambda(C)$ or $\Lambda({}_{n-1}S)$; rather, one computes $LogL_C = ln(\Lambda(C))$ and $LogL_{{}_{n-1}S} = ln(\Lambda({}_{n-1}S))$, and then sets ${}_nR = exp\left(LogL_C - LogL_{{}_{n-1}S}\right)$.

The classical result Hastings (1970) is that in the limit as $N \to \infty$ this algorithm yields a sample from the posterior density.

A.2.2. Priors

The bounds of the uniform densities one uses to define the priors matter very little provided they are sufficiently inclusive so as not to cut off any part of the posterior density. In the current simulations, the prior densities of all parameters that could take signed values were uniform between −1000 and 1000, and the prior densities on all parameters that were required to be nonnegative were uniform between 0 and 1000. As candidate parameter vectors C were drawn, the program checked to make sure that each coordinate value C_k was within the upper and lower boundaries of its prior density.

A.2.3. Adaptive candidate selection

As noted above, on the nth iteration of the MCMC process, one randomly selects a candidate parameter vector C in the neighborhood of ${}_{n-1}S$. The window used to perform this sampling (i.e., how one defines the sampling neighborhood) dramatically influences the efficiency with which one can estimate the posterior joint density of the parameters. This sampling window is adjusted adaptively after each 2000 iterations of the MCMC process. Specifically, let S_{last2000} be the matrix whose columns are the 2000 most recent parameter vectors added to the list by the MCMC process. In each of the subsequent 2000 iterations of the MCMC process, each successive candidate parameter vector ${}_kC$ is drawn by setting ${}_kC = {}_{k-1}S + X$ where the vector $X = (X_1, X_2, X_{N_{params}})$ comprises independent normal random variables, where $E[X_j] = 0$ and the standard deviation of X_j is $\frac{\sigma_j}{3}$ for σ_j the standard deviation of the jth column of S_{last2000}. This method succeeds in achieving an MCMC process that moves efficiently to scribble in the joint posterior density.

A.2.4. Starting values, burn-in, and number of iterations

For each of the models evaluated in this paper, several starting points were tested. In all cases, results were robust with respect to these variations. For the basic seed expansion model, results were stable after 10,000 iterations. We typically collected 20,000 iterations and retained the last 10,000 samples to estimate the posterior density. For the 3D4C model, more samples were required. In each run, 300,000 iterations were observed, and the last 100,000 were retained to estimate the posterior density.

[6] If the prior density f_{prior} were nonuniform, then we would have ${}_nR = \frac{\Lambda(C)f_{prior}(C)}{\Lambda({}_{n-1}S)f_{prior}({}_{n-1}S)}$.

References

Adelson, E. H., & Bergen, J. R. (1991). The plenoptic function and the elements of early vision. In M. S. Landy & J. A. Movshon (Eds.), *Computational models of visual processing* (pp. 3–20). Cambridge, MA: MIT Press.

Baud-Bovy, G., & Soechting, J. (2001). Visual localization of the centre of mass of compact, asymmetric, two-dimensional shapes. *Journal of Experimental Psychology: Human Perception and Performance, 27*, 692–706.

Blackwell, H. R. (1946). Contrast thresholds of the human eye. *Journal of the Optical Society of America, 36*, 624–643.

Bowen, R. W., Pokorny, J., & Smith, V. C. (1989). Sawtooth contrast sensitivity: Decrements have the edge. *Vision Research, 29*, 1501–1509.

Chan, H., & Tyler, C. W. (1992). Increment and decrement asymmetries: Implications for pattern detection and appearance. *Society for Information Display Symposium Digest, 23*, 251–254.

Chubb, C., Darcy, J., Landy, M. S., Econopouly, J., Nam, J-H., & Sperling, G. (in press). The scramble illusion: Texture metamers. In A. Shapiro & D. Todorovic (Eds.), *Oxford compendium of visual illusions*. Oxford University Press. in press.

Chubb, C., Econopouly, J., & Landy, M. S. (1994). Histogram contrast analysis and the visual segregation of iid textures. *Journal of the Optical Society of America A, 11*, 2350–2374.

Chubb, C., & Landy, M. S. (1991). Orthogonal distribution analysis: A new approach to the study of texture perception. In M. S. Landy & J. A. Movshon (Eds.), *Computational models of visual processing* (pp. 291–301). Cambridge, MA: MIT Press.

Chubb, C., Landy, M. S., & Econopouly, J. (2004). A visual mechanism tuned to black. *Vision Research, 44*, 3223–3232.

Chubb, C., & Nam, J.-H. (2000). The variance of high contrast texture is sensed using negative half-wave rectification. *Vision Research, 40*, 1695–1709.

Chubb, C., Nam, J-H., Bindman, D. R., & Sperling, G. (2007). The three dimensions of human visual sensitivity to first-order contrast statistics. *Vision Research, 47*, 2237–2248.

Chubb, C., Scofield, I., Chiao, C.-C., & Sperling, G. (2012). A method for analyzing the dimensions of preattentive visual sensitivity. *Journal of Mathematical Psychology, 56*, 427–443.

Dannemiller, J. L., & Stephens, B. R. (2001). Dannemiller jl, stephens br (2001) asymmetries in contrast polarity processing in young human infants. *Journal of Vision, 1*, 112–125.

Friedenberg, J., & Liby, B. (2002). Perception of two-body center of mass. *Perception and Psychophysics, 64*, 530–539.

Hastings, W. K. (1970). Monte Carlo sampling methods using Markov chains and their applications. *Biometrika, 57*, 97–109.

Hoel, P. G., Port, S. C., & Stone, C. J. (1971). *Introduction to statistical theory*. Boston, MA: Houghton-Mifflin.

Jin, J., Wang, Y., Lashgari, R., Swadlow, H. A., & Alonso, J-M. (2011). Faster thalamocortical processing for dark than light visual targets. *The Journal of Neuroscience, 31*(48), 17471–17479.

Komban, S. J., Alonso, J.-M., & Zaidi, Q. (2011). Darks are processed faster than lights. *The Journal of Neuroscience, 31*(23), 8654–8658.

Konstevich, L. L., & Tyler, C. W. (1999). Nonlinearities of near-threshold contrast transduction. *Vision Research, 39*, 1869–1880.

Krauskopf, J. (1980). Discrimination and detection of changes in luminance. *Vision Research, 20*, 671–677.

Lu, Z.-L., & Sperling, G. (2012). Black–white asymmetry in visual perception. *Journal of Vision, 12*(10:8), 1–21.

McGowan, J. W., Kowler, E., Sharma, A., & Chubb, C. (1998). Saccadic localization of random dot targets. *Vision Research, 38*, 895–909.

Nam, J-H., & Chubb, C. (2000). Texture luminance judgments are approximately veridical. *Vision Research, 40*, 1677–1694.

Robson, J. G. (1980). Neural images: The physiological basis of spatial vision. In C. S. Harris (Ed.), *Visual coding and adaptability* (pp. 177–214). Hillsdale, NJ: Erlbaum.

Short, A. D. (1966). Decremental and incremental visual thresholds. *Journal of Physiology, 185*, 646–654.

Treisman, A. M., & Gelade, G. (1980). A feature-integration theory of attention. *Cognitive Psychology, 12*, 97–136.

Treisman, A. M., & Gormican, S. (1988). Feature analysis in early vision: Evidence from search asymmetries. *Psychological Review, 95*, 15–48.

Victor, J. D., Chubb, C., & Conte, M. M. (2005). Interaction of luminance and higher order statistics in texture discrimination. *Vision Research, 45*, 311–328.

Whittle, P. (1986). Increments and decrements: Luminance discrimination. *Vision Research, 26*, 1677–1691.

Wilks, S. S. (1938). The large-sample distribution of the likelihood ratio for testing composite hypotheses. *The Annals of Mathematical Statistics, 9*, 60–62.

Xing, D., Yeh, C. I., & Shapley, R. M. (2010). Generation of black-dominant responses in v1 cortex. *The Journal of Neuroscience, 30*(40), 13504–13512.

Yeh, C. I., Xing, D., & Shapley, R. M. (2009). Black responses dominate macaque primary visual cortex v1. *The Journal of Neuroscience, 29*, 11753–11760.